RSC Advances

PAPER

View Article Online
View Journal | View Issue



Cite this: *RSC Adv.*, 2025, **15**, 25771

# High performance self-assembled pyrene-based emitter with narrowband emission and excellent luminescence efficiency†

Zhongxing Geng, *[a] Zhentan Wang,[a] Hailong Liu,[a] Xiangyi Su,[a] Liangyu Hu,[a] Fengyan Song [c] and Kun Yao *[b]

Received 22nd May 2025
Accepted 14th July 2025

DOI: 10.1039/d5ra03596a

rsc.li/rsc-advances

To address the problem of broad emission spectra of organic luminescent materials, a novel and effective molecular design strategy is presented to reduce the full width at half maximum (FWHM) of emission by integrating the multi resonance (MR) B–N moiety into the pyrene-based backbone system, named **DtBuCzB-Py**. Taking advantages of BN-core in narrowband emission and planar rigid structure, the obtained compound **DtBuCzB-Py** not only exhibited narrowband emission (FWHM = 25 nm in toluene solution; FWHM = 38 nm in spin-coated film) and high fluorescence quantum yield ($\Phi_F$ = 77.2% in toluene solution; $\Phi_F$ = 36.8% in spin-coated film), but also strong self-assembly ability.



Highly efficient organic luminescent materials with narrowband emission have garnered significant interest in recent years owing to their wide range of potential applications in high-resolution organic optoelectronic display devices.[1,2] Unfortunately, because of the vibrational coupling between the ground state and the excited state as well as the structural relaxation in the excited state, the emission spectra of traditional fluorescence emitters exhibit an inherent broadband emission with full width at half-maximum (FWHM), resulting in a relatively low color purity.[3,4] Moreover, most organic luminescent materials suffer from an unfavorable aggregation-caused quenching (ACQ) effect, which significantly limits their practical application requirements.[5,6] Therefore, it is a great challenge to achieve organic luminescent materials that exhibit both narrow-band emission (less than 50 nm) and high luminescence efficiency.

Pyrene and its derivatives, one of the most important blue-coloured chromophores and supramolecular self-assembly moieties, have been widely applied for various optoelectronic devices due to their conjugated structure, long fluorescence lifetime, and high luminous efficiency.[7–9] Due to the planar π-conjugated molecular structure, pyrene is more inclined to form dimers through strong π–π stacking interactions in the aggregated or film state, resulting in corresponding redshift emissions and reducing the fluorescence quantum yield ($\Phi_F$).[10–12] To overcome the nature of the ACQ effect, one of the most commonly used strategies is to functionalize the pyrene core by introducing chromophores with aggregation-induced luminescence (AIE) characteristics to achieve novel pyrene-based AIE luminogens (AIE gens) with considerable luminous efficiency.[13–15] For instance, Tang and his collaborators synthesized an asymmetrical tetraphenylethylene (TPE)-substituted pyrene with AIE characteristics, where blue emission of naked TPE and yellow emission of diethylaminophenyl-substituted TPE units were introduced at the 2- and 7-positions of pyrene, respectively.[16] Interestingly, the resulting asymmetric compound not only displays a tunable AIE emission from blue (435 nm) to warm white (dual emission: 436 nm and 538 nm), but also exhibits a high luminous efficiency ($\Phi_F$ = 22%). However, like most organic luminescent materials, the traditional pyrenes show a broad emission under irradiation. In particular, the pyrene-based AIEgens containing twisted confirmations tend to exhibit bright emissive properties with wider FWHM, due to the diversity of excited-state structural relaxation.[4] Thus, developing high-performance pyrene emitters with both narrowband emission and high photoluminescence efficiency is a meaningful but challenging task.

Since Hatakeyama *et al.* pioneered the multi resonance (MR) molecules with narrowband emission to improve the color purity of organic light-emitting diodes (OLEDs) in 2016, MR molecules have received extensive attention for the development of high-performance organic functional materials and devices.[17–25] Consequently, combining the advantages of MR molecules with narrowband emission and the pyrene core with tunable planar rigidity structure is the promising candidate strategy to overcome the challenge of pyrene luminescent

[a]School of Energy, Materials and Chemical Engineering, Hefei University, Hefei, Anhui, 230601, China. E-mail: gzx@hfuu.edu.cn

[b]School of Chemical and Printing-Dyeing Engineering, Henan University of Engineering, Zhengzhou, Henan, 450007, China. E-mail: yaokun0820@163.com

[c]College of Chemistry and Life Science, Beijing University of Technology, Beijing 100124, China

† Electronic supplementary information (ESI) available. See DOI: https://doi.org/10.1039/d5ra03596a

material with narrowband emission and high photoluminescence efficiency, especially in the film state. In this work, a novel pyrene-based emitter **DtBuCzB-Py** was successfully synthesized by incorporating a multi-resonance (MR) B–N moiety into the pyrene-based backbone through the Suzuki coupling reaction (Scheme 1). It was found that the obtained **DtBuCzB-Py** not only exhibited narrowband emission (FWHM = 25 nm in toluene solution; FWHM = 38 nm in spin-coated film) and high fluorescence quantum yield ($\Phi_F$ = 77.2% in toluene solution; $\Phi_F$ = 36.8% in spin-coated film), but also possessed strong assembly ability. Notably, the $\Phi_F$ value of **DtBuCzB-Py** in both solution and spin-coated film states can be maintained at a relatively high level compared with the reported pyrene-based emitters.[9,11,16] This work presents a novel molecular design strategy that can simultaneously achieve narrowband emission, high luminescence efficiency, and strong self-assembly ability of pyrene-based emitters.

The target compound **DtBuCzB-Py** was synthesized through a Suzuki coupling reaction and the detailed procedures and characterization data of **DtBuCzB-Py** are listed in the ESI.† The thermal stability of **DtBuCzB-Py** was evaluated by thermogravimetric analysis (TGA) under a nitrogen atmosphere with a heating rate of 10 °C $min^{-1}$. As depicted in Fig. S1,† the degradation temperatures ($T_d$) corresponding 5% weight loss exceeds 419.4 °C, indicating good thermal stability. Moreover, **DtBuCzB-Py** exhibits excellent solubility in common solvents, such as dichloromethane ($CH_2Cl_2$), tetrahydrofuran (THF), and toluene, which is conducive to the formation of high-quality films by spin-coating.

The UV-Vis absorption and photoluminescence (PL) emission spectra of **DtBuCzB-Py** were investigated in both dilute toluene ($1 \times 10^{-5}$ mol $L^{-1}$) and spin-coated states (SI). As shown in Fig. 1, **DtBuCzB-Py** exhibits dominant long-wavelength absorption bands at around 369 nm in toluene solution and 381 nm in spin-coated film, respectively, which can be regarded as the $n$–$\pi$* transition in the pyrene system.[26,27] Additionally, the strong absorption band of **DtBuCzB-Py** that appears near 470 nm can be attributed to the BN moiety.[20] Moreover, similar PL bands of **DtBuCzB-Py** can be observed at around 487 nm in toluene solution and 504 nm in spin-coated film, with the CIE coordinates of (0.08, 0.34) and (0.21, 0.61), respectively

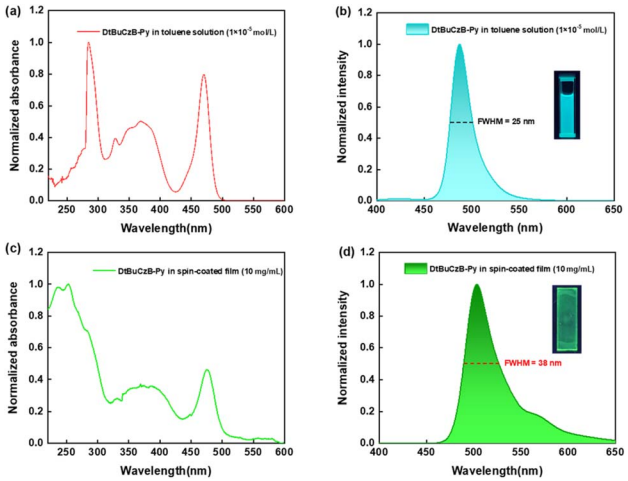


Fig. 1 (a) UV-Vis absorption and (b) fluorescent emission spectra of **DtBuCzB-Py** in toluene solution ($\lambda_{ex}$ = 365 nm); (c) UV-Vis absorption and (d) fluorescent emission spectra of **DtBuCzB-Py** in spin-coated film ($\lambda_{ex}$ = 365 nm). Inset color images: photograph of **DtBuCzB-Py** in the toluene solution and spin-coated film under UV illumination (365 nm).

(Fig. S2†). To our delight, by integrating the B–N moiety into the pyrene-based backbone, the **DtBuCzB-Py** can exhibit narrowband emission in both toluene solution and spin-coated film, with FWHM values of 25 nm and 38 nm, respectively. This indicated that the B–N moiety has effectively suppressed the intramolecular interaction and fixed the molecular motion of pyrene core in the film state, resulting in a narrowed FWHM emission. The fluorescence quantum yield ($\Phi_F$) of **DtBuCzB-Py** in THF solution and spin-coated film was 77.2% (fluorescence lifetime: $\tau$ = 8.6 ns, Fig. S3a†) and 36.8% ($\tau$ = 2.2 ns, Fig. S3b†), respectively, indicating that this novel pyrene-based emitter achieves both narrowband emission and high $\Phi_F$, simultaneously. Notably, the fluorescence lifetimes of **DtBuCzB-Py** in spin-coated films at 77 K and 300 K are close, both at the ns level (Fig. S4†), indicating that it belongs to the fluorescent emission rather than thermally activated delayed fluorescence (TADF). Furthermore, the THF/water mixed solvent PL tests demonstrate that the decrease in the PLQY value of **DtBuCzB-Py** can be

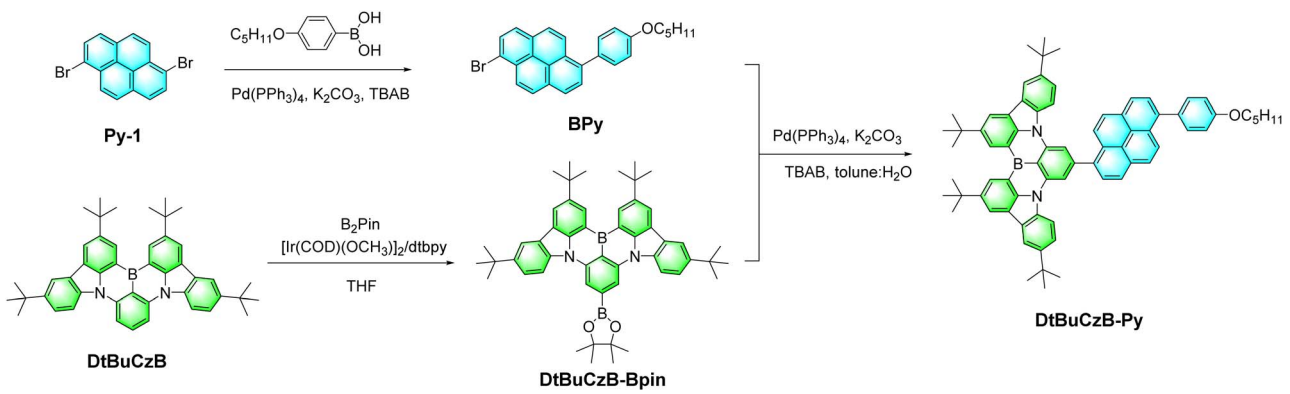


Scheme 1 The synthetic routes of BN-core pyrene-based emitter **DtBuCzB-Py**.

attributed to the ACQ effect caused by the π–π stacking interactions of pyrene emitters in the aggregated or spin-coated film state (Fig. S5†).

It is well known that pyrene-based luminescent molecules usually have good assembly ability due to their rigid planar molecular structure.[28–32] To deeply study the self-assembly ability of the **DtBuCzB-Py**, its morphology under different conditions was characterized by scanning electron microscopy (SEM). As presented in Fig. 2, at film concentration of 10 mg $mL^{-1}$, 0.1 mg $mL^{-1}$, and $1 \times 10^{-3}$ mg $mL^{-1}$, **DtBuCzB-Py** forms a sheet-like morphology. Interestingly, the morphology of **DtBuCzB-Py** in the aggregated state ($1 \times 10^{-3}$ mg $mL^{-1}$, THF/$H_2O$ = 80/20, v/v) changes from twisted sheet-like to regular fibrous structure, indicating that it has good self-assembly ability in both the film and the aggregated states. The regular fibrous morphology of **DtBuCzB-Py** possibly originates from the planar rigid molecular of pyrene-core, which can form ordered molecular arrangements driven by π–π stacking interactions.

X-ray diffraction (XRD) patterns and 2D grazing incidence wide-angle X-ray scattering (2D-GIWAXS) were employed to clarify the possible molecular packing mode of **DtBuCzB-Py**. As depicted in Fig. 3, **DtBuCzB-Py** shows the broad characteristic diffraction peaks of pyrene-based emitters in both powder and spin-coated films. It should be noted that the powder and spin-coated film of **DtBuCzB-Py** exhibited similar diffraction peaks, and the two main diffraction peaks were centered at $2\theta$ = 5.7°/17.6° and 4.9°/21.8°. Moreover, their corresponding distances were calculated to be 1.55/0.50 nm and 1.80/0.40 nm according to the Bragg's equation. Among them, **DtBuCzB-Py** spin-coated film with a *d*-spacing of 0.40 nm could be attributed to the ordered π–π stacking.[33,34] Meanwhile, the 2D GIWAXS pattern of **DtBuCzB-Py** spin-coated film consists of two rings at $q_{xy}$ = 0.49 and 1.44 $Å^{-1}$ (Fig. 4a and b), corresponding to *d*-spacings of 12.8 and 4.4 Å, respectively, which matches well with the XRD pattern. The results of XRD and 2D GIWAXS confirm that π–π

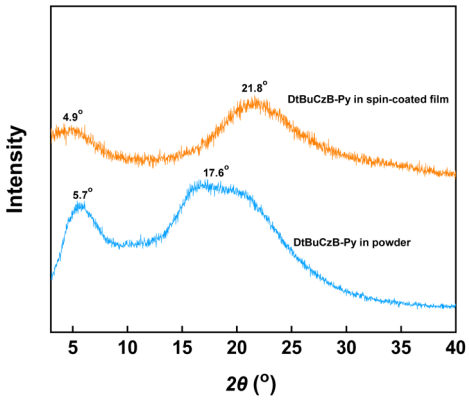


Fig. 3 XRD patterns of **DtBuCzB-Py** in powder and spin-coated film.

stacking interactions are the driving force for the ordered assembly of **DtBuCzB-Py**. Furthermore, the morphology of spin-coated film of **DtBuCzB-Py** was also studied by atomic force microscopy (AFM). As shown in Fig. 4c, the root mean square (RMS) roughness value of **DtBuCzB-Py** film was 0.93 nm, which further confirmed the existence of regular and ordered self-assembly, and also indicate the good film-forming ability.

The optimized molecular geometry and the electronic properties of **DtBuCzB-Py** in the ground state were performed by density functional theory (DFT) calculations at the B3LYP-D3BJ/6-31G (d) level using the Gaussian 16 program. As displayed in Fig. 5, the highest occupied molecular orbital (HOMO), the lowest unoccupied molecular orbital (LUMO), and the energy gap levels ($E_g$) of **DtBuCzB-Py** were calculated to be −5.00 eV, −1.8 eV, and 3.20 eV, respectively. Notably, the electron density of the HOMO is localized on the BN-moiety, while the electron density of the LUMO is mainly located on the pyrene-core. The clear separation between the HOMO and LUMO levels is beneficial for efficient carrier injection and transport. The DFT calculation of **DtBuCzB-Py** in the excited state has also been

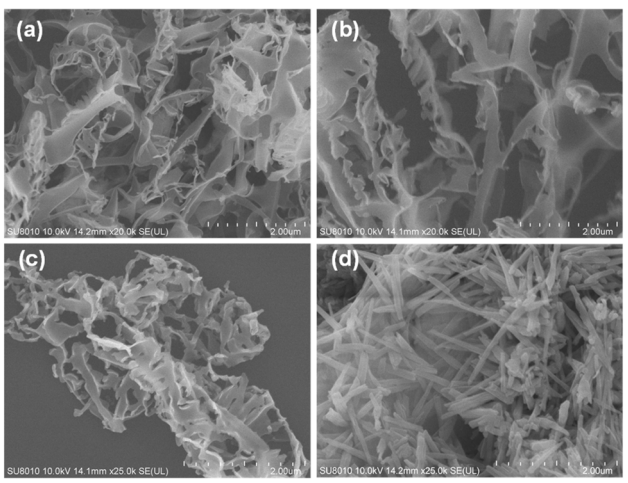


Fig. 2 SEM images of **DtBuCzB-Py**: (a) in film (10 mg $mL^{-1}$ in toluene), (b) in film (0.1 mg $mL^{-1}$ in toluene), (c) in film ($1 \times 10^{-3}$ mg $mL^{-1}$ in toluene), and (d) in aggregated state ($1 \times 10^{-3}$ mg $mL^{-1}$, THF/$H_2O$ = 80/20, v/v).

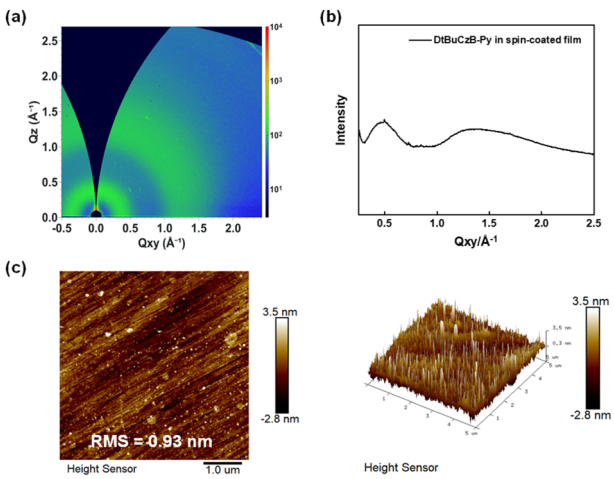


Fig. 4 (a) 2D GIWAXS pattern of **DtBuCzB-Py** spin-coated film; (b) 1D GIWAXS curve of **DtBuCzB-Py** spin-coated film; (c) AFM top and 3D images (5 × 5 $\mu m^2$) of **DtBuCzB-Py** in the spin-coated film.

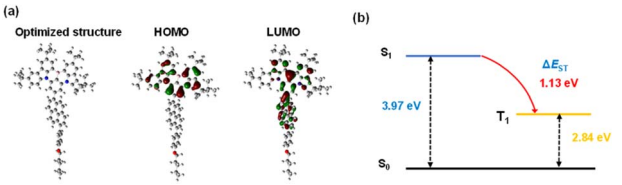


Fig. 5 (a) Optimized structures and calculated HOMO–LUMO spatial distributions of **DtBuCzB-Py**; (b) the $S_1$, $T_1$, and $\Delta E_{ST}$ energy levels of **DtBuCzB-Py** in the excited state.

performed (Fig. 5b). The calculated $S_1$, $T_1$, and $\Delta E_{ST}$ energy levels of **DtBuCzB-Py** are 3.97, 2.84, and 1.13 eV, respectively. Moreover, we have also collected the fluorescence and phosphorescence spectra of **DtBuCzB-Py** in spin-coated films under liquid nitrogen (77 K). As shown in Fig. S6,† the measured $S_1$, $T_1$ and $\Delta E_{ST}$ energy levels are 2.72 eV, 2.28 eV, and 0.44 eV, respectively. The large $\Delta E_{ST}$ confirm that **DtBuCzB-Py** is a common fluorescent emission dye.[35]

In summary, we propose a simple yet efficient design strategy to narrow the pyrene-based emitters with high luminescence efficiency by integrating the multi resonance (MR) B–N moiety into the pyrene-based backbone. Interestingly, the obtained compound **DtBuCzB-Py** exhibited narrowband emission (FWHM = 25 nm in toluene solution; FWHM = 38 nm in spin-coated film) and high fluorescence quantum yield ($\Phi_F$ = 77.2% in toluene solution; $\Phi_F$ = 36.8% in spin-coated film). Moreover, due to the assembly ability of pyrene core and the planar rigidity of BN-moiety, **DtBuCzB-Py** can self-assemble into a regular fibrous structure. This work proposes a novel molecular design strategy to achieve narrowband emission, high luminescence efficiency, and strong self-assembly ability of pyrene-based emitters, simultaneously.

## Data availability

All data generated or analysed during this study are included in this published article and its ESI.†

## Author contributions

Zhongxing Geng: conceptualization, methodology, investigation, and writing – original draft. Zhentan Wang, Hailong Liu, and Xiangyi Su: investigation and data analysis. Liangyu Hu and Fengyan Song: formal analysis, and writing – review & editing. Kun Yao: supervision, validation, and funding acquisition.

## Conflicts of interest

There are no conflicts to declare.

## Acknowledgements

This work was supported by the Anhui Provincial Natural Science Foundation (2308085QB59), National Natural Science Foundation of China (22305059 and 22303028), and the University Natural Science Research Project of Anhui Province (2024AH051501).

## Notes and references

1 G. Hong, X. Gan, C. Leonhardt, Z. Zhang, J. Seibert, J. M. Busch and S. Bräse, *Adv. Mater.*, 2021, **33**, 2005630.
2 Y. Huang, M. Jia, C. Li, Y. Yang, Y. He, Y. J. Luo, Y. Huang, L. Zhou and Z. Lu, *Chem. Commun.*, 2024, **60**, 3194.
3 M. H. Jung, H. H. Seon, P. Ambika, J. E. Jeong and H. Y. Woo, *NPG Asia Mater.*, 2021, **13**, 53.
4 X. Feng, X. Wang, C. Redshaw and B. Z. Tang, *Chem. Soc. Rev.*, 2023, **52**, 6715–6753.
5 Y. Wang, L. Cui, Y. Wang, F. Li, Y. Li and Q. Meng, *Chem. Eur. J.*, 2023, **29**, e202302373.
6 Q. Meng, L. Cui, Q. Liao, J. Xu and Y. Wang, *Chem. Commun.*, 2022, **58**, 10384–10387.
7 K. Takaishi, S. Murakami, K. Iwachido and T. Ema, *Chem. Sci.*, 2021, **12**, 14570–14576.
8 O. A. Krasheninina, D. S. Novopashina, E. K. Apartsin and A. G. Venyaminova, *Molecules*, 2017, **22**, 2108.
9 W. Liu, S. Li, Z. Xie, K. Huang, K. Yan, Y. Zhao, C. Redshaw, X. Feng and B. Z. Tang, *Adv. Opt. Mater.*, 2024, **12**, 2400301.
10 D. Niu, Y. Jiang, L. Ji, G. Ouyang and M. Liu, *Angew. Chem., Int. Ed.*, 2019, **58**, 5946–5950.
11 A. K. Swain, K. Kolanji, C. Stapper and P. Ravat, *Org. Lett.*, 2021, **23**, 1339–1343.
12 Q. Cheng, A. Hao and P. Xing, *ACS Nano*, 2024, **18**, 5766–5777.
13 M. M. Islam, Z. Hu, Q. Wang, C. Redshaw and X. Feng, *Mater. Chem. Front.*, 2019, **3**, 762–781.
14 J. Y. Cao, G. Yang, Z. M. Xue, W. X. Zhao, S. H. Chen, H. T. Lin, T. Yamato, C. Redshaw, D. Y. Gu and C. Z. Wang, *Dyes and Pigm.*, 2023, **220**, 111758.
15 E. V. Varghese, C. Y. Yao and C. H. Chen, *Chem. – Asian J.*, 2024, **19**, e202300910.
16 X. Feng, C. Qi, H. T. Feng, Z. Zhao, H. H. Y. Sung, I. D. Williams, R. T. K. Kwok, J. W. Y. Lam, A. Qin and B. Z. Tang, *Chem. Sci.*, 2018, **9**, 5679–5687.
17 T. Hatakeyama, K. Shiren, K. Nakajima, S. Nomura, S. Nakatsuka, K. Kinoshita, J. Ni, Y. Ono and T. Ikuta, *Adv. Mater.*, 2016, **28**, 2777.
18 Y. Xu, Q. Wang, X. Cai, C. Li and Y. Wang, *Adv. Mater.*, 2021, **33**, 2100652.
19 W. Luo, T. Wang, Z. Huang, H. Huang, N. Li and C. Yang, *Adv. Funct. Mater.*, 2024, **34**, 2310042.
20 K. K. Tan, W. C. Guo, L. Zhao, W, M. Li and C. F. Chen, *Angew. Chem., Int. Ed.*, 2024, **63**, e202412283.
21 C. H. Guo, Y. Zhang, W. L. Zhao, K. K. Tan, L. Feng, L. Duan, C. F. Chen and M. Li, *Adv. Mater.*, 2024, **36**, 2406550.
22 Y. Huo, H. Qi, S. He, J. Li, S. Song, J. Lv, Y. Liu, L. Peng, S. Ying and S. Yan, *Aggregate*, 2023, **4**, e391.
23 Y. Wang, Z. Ma, J. Pu, D. Guo, G. Li, Z. Chen, S. J. Su, H. Deng, J. Zhao and Z. Chi, *Aggregate*, 2024, **5**, e585.
24 X. F. Luo, S. Q. Song, X. Wu, C. F. Yip, S. Cai and Y. X. Zheng, *Aggregate*, 2024, **5**, e445.

25 J. Wang, H. Hafeez, S. Tang, T. Matulaitis, L. Edman, I. D. Samuel and E. Zysman-Colman, *Aggregate*, 2024, **5**, e571.
26 S. Zhang, Y. Sheng, G. Wei, Y. Quan, Y. Cheng and C. Zhu, *Polym. Chem.*, 2015, **6**, 2416–2422.
27 Y. Zhang, Z. Geng, Y. Zhang, Z. Xu, H. Li, Y. Cheng and Y. Quan, *J. Phys. Chem. Lett.*, 2021, **12**, 3767–3772.
28 T. M. Figueira-Duarte and K. Müllen, *Chem. Rev.*, 2011, **111**, 7260–7314.
29 Y. Zhang, H. Li, Z. Geng, W. Zheng, Y. Quan and Y. Cheng, *Nat. Commun.*, 2022, **13**, 4905.
30 H. Shigemitsu, K. Kawakami, Y. Nagata, R. Kajiwara, S. Yamada, T. Mori and T. Kida, *Angew. Chem., Int. Ed.*, 2022, **61**, e202114700.
31 S. Yang, F. Li, Q. Li, J. Han and Y. Cheng, *ACS Appl. Opt. Mater.*, 2023, **1**, 1492–1500.
32 S. Yang, F. Hu, T. Xu, F. Lin, J. Han and F. Li, *Chem. Eur. J.*, 2024, **30**, e202402012.
33 P. Qin, Z. Wu, P. Li, D. Niu, M. Liu and M. Yin, *ACS Appl. Mater. Interfaces*, 2021, **13**, 18047–18055.
34 M. Ma, A. Hao and P. Xing, *Nanoscale*, 2022, **14**, 8163–8171.
35 D. Wan, J. Zhou, Y. Yang, G. Meng, D. Zhang, L. Duan and J. Ding, *Adv. Mater.*, 2024, **36**, 2409706.